PREPARATION AND NITROBENZENE REACTION KINETICS OF MICROCRYSTALLINE TUNGSTEN BRONZE THIN FILMS WITH OR WITHOUT TRANSITION METAL (Ag, Ti, Cr, Mn, Fe, Co, Ni and Cu) COATINGS.

By

KASHIF RASHID KHAN

Bachelors of Science in Chemistry

University of the Punjab

Lahore, Pakistan

1999

Submitted to the Faculty of the
Graduate College of the
Oklahoma State University
in partial fulfillment of
the requirements for
the Degree of
MASTERS OF SCIENCE
May, 2006

PREPARATION AND NITROBENZENE REACTION

KINETICS OF MICROCRYSTALLINE

TUNGSTEN BRONZE THIN FILMS WITH OR

WITHOUT TRANSITION METAL

(Ag, Ti, Cr, Mn, Fe, Co, Ni and Cu)

COATINGS

Thesis Approved:

Dr. Nicholas F. Materer

Thesis Adviser

Dr. Stacy D. Benson

Dr. Allen W. Apblette

Dr. A. Gordon Emslie

Dean of the Graduate College

ACKNOWLEDGEMENTS

All the praises for almighty God, the most beneficent and the most merciful. He guides us in darkness and helps in difficulties. All the thanks to God almighty, who is the entire source of knowledge and wisdom endowed to making and for equipping humble creatures with mental facility. All the respects and gratitude for Holy Prophet Muhammad (Peace be upon him) who is for even a blessing a torch of guidance and light of knowledge for mankind and teaches us high ideas of life.

I feel great pleasure in expressing my profound and cordial gratitude to my respected teachers and learned supervisor Dr. Nicholas F. Materer for his admirable co-operation, inspiration, encouragement, skilled guidance and sympathetic attitude which enabled me to handle most of the problems successfully. His constructive, sympathetic and frank attitude has painted a deep and everlasting impression on the pages of my life. I feel gratitude for his so long as whole life of mine.

I would also like to thank to members of my graduate committee, Dr Allen W. Apblett and Dr Stacy D. Benson. Their deduction to research and teaching has helped open my mind and has helped me learning experience to become a better researcher.

I am thankful and highly obliged to honorable Dr. Neil Purdie chairman of the Chemistry Department for his kind and helpful attitude.

I would like to thank Dane Scott for his help in the laboratory and making it a more pleasant place to work.

I would like to thank the Department of Chemistry for providing me a teaching assistantship for support during my graduate work at OSU. I would also like to express my appreciation to Carolyn, Bob and Cheryl in the Chemistry Department office for their assistant over the last few years.

Finally, I would like to express my greatest gratitude to my friends and family, especially to my mother. Their continued support for the past few years has been of great help to me in finishing this project.

TABLE OF CONTENTS

LIST OF TABLES

LIST OF FIGURES

LIST OF SYMBOLS AND ABBREVIATIONS

b	Reaction rate
C	Concentration
C_H	Hydrogen Concentration
const	Constant
C_{ox}	Oxidant Concentration
D	Diffusion coefficient
d	Thickness
E_F	Fermi level
E_{rel}	Relative energy
F	Deposition rate
FWHM	Full Width at Half Maximum
I	Absorbance intensity
i	Current
IRC	Internal Reaction Coordinate
k	Reaction constant
L	Film thickness
M	Molecular weight
n	Number of moles

NB	Nitrobenzene
NMR	Nuclear Magnetic Resonance
PES	Synchrotron Radiation Photoemission Spectroscopy
R	Interatomic distance
S	Number of surface sites
SEM	Scanning Electron Microscopy
STM	Scanning Tunneling Microscopy
T	Temperature
t	Time
TS	Transition State
U	Potential
UHV	Ultra-High Vacuum
UV-Vis	Ultraviolet-Visible (Spectroscopy)
XPS	X-Ray Photoelectron Spectroscopy
XRD	X-Ray Diffraction
λ	Wavelength
ρ	Density
θ	Surface coverage
τ	Relaxation time

CHAPTER I

INTRODUCTION TO

TUNGSTEN HYDROGEN BRONZES

A. Tungsten trioxide and tungsten trioxide bronze thin films.

Our interest in tungsten trioxide (WO_3) and hydrogen tungsten trioxide bronze (H_xWO_3) stems from their ability to act as a safe source of hydrogen. Early work in Dr. Allen W. Apblett's research group at Oklahoma State University has shown that these compounds can also react with organic substances such as tetrachloromethane resulting in the formation of chloroform.[1,2] More importantly, hydrogen tungsten trioxide bronze can react with nitro-containing compounds yielding amines. Thus, this compound has potential applications in detecting and decapacitating explosives. The figure above illustrates a potential scheme. Hydrogen (H) atoms diffuse from the bronze to the surface and react with the nitro compounds, possibly at a catalytic site formed by metal deposition. Another reaction with the solvent can regenerate the bronze. To realize this system, several things need to be examined (1) reactivity of the bronze (2) diffusion of H atoms to the surface and (3) effect of the deposited metal on the surface.

Chapter I contains a brief review of the mechanism of coloration and bleaching of tungsten trioxide films along with some structural properties. Tungsten trioxide reversibly changes its optical properties when reduced to bronze.

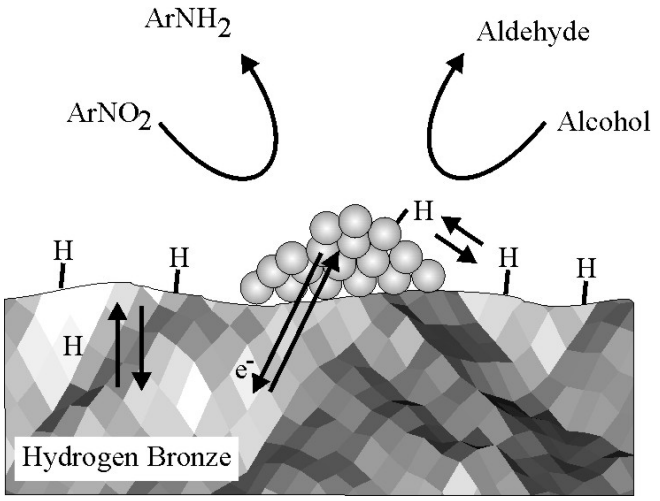

Figure I-1. Formation of hydrogen bronze and its reaction with some oxidizing compounds.

Chapter II is devoted to the review of preparation and properties of tungsten trioxide (WO_3) and tungsten trioxide hydrogen bronze (H_xWO_3) without a catalyst. The reaction kinetics of tungsten bronzes with nitrobenzene solution, studied by ultraviolet visible spectroscopy, is described in chapter III. Here an appropriate kinetic model is developed and fitted to the experimental data. Due to such an approach both the reaction constant and the hydrogen diffusion coefficient of tungsten bronze thin films can be determined. These parameters are significant for manufacturing explosive deactivation devices because they relate the actual concentration of nitro-containing compounds with the optical properties of tungsten bronze films. The value of the diffusion coefficient is compared with the results obtained previously by NMR study of hydrogen transport in tungsten oxide thin films. Catalyst activators on WO_3 thin films such as Pt, Pd, Rh, Au, and Ag are reported in the litrature.[1-5] This enhances both sensitivity and selectivity of WO_3 thin films and some other metal oxide[4] systems. They are also extensively used for

making gas sensors,[3-6] smart windows,[11,12] displays,[13,14] and rear view mirrors.[15] So in the next chapter of this work the preparation, properties and reaction kinetics of silver coated tungsten bronzes is studied with nitrobenzene. First silver is deposited on WO_3 surfaces and then the effect of silver concentration on the rate of reduction of nitrobenzene is studied for samples prepared by using different percentages of hydrogen in the tungsten bronze. Finally the effect of deposition of first row transition metals, titanium, chromium, manganese, iron, cobalt, nickel and copper on WO_3 film surfaces on reaction rate is studied.

.

B. Coloration of hydrogen tungsten bronze

Tungsten trioxide is an N type semiconductor that has received intensive attention in recent years due to its ability to reversibly change color from yellow (WO_3) to deep blue (bronzes M_xWO_3, M=H, Li, K etc) under the influence of external parameters, such as temperature, irradiation or applied voltage or exposure to a particular gas.[3-7] This results in their usefulness in a variety of applications, which include gas sensors,[3-6] smart windows,[11,12] displays,[13,14] and rear view mirrors.[15] The use of a catalyst on WO_3 surface has also gained importance due to enhancement in sensitivity of the films to a particular gas.[3-6] The preparation techniques for WO_3 films include sputtering in $Ar+O_2$ plasma,[16-18] chemical vapor deposition,[19,21] plasma-enhanced chemical vapor deposition,[22] anodic oxidation,[23,24] sol-gel-derived films,[25-27] decomposition of oxalatotungstate compounds,[26] electro-deposition,[28] thermal oxidation[29] and hydrothermal treatment.[30] The structural properties, as well as optical and electrical behaviors of the film depend on the deposition method.

Different models were proposed to explain the optical absorption in colored tungsten bronze thin films. Earlier work on the properties of the colored WO_3 formed by optical and electrical excitation suggested a model involving trapping electrons in oxygen ion vacancies.[31] It can be supported by the fact that as soon as the color centers have been bleached by heating in oxygen at high temperature they cannot be regenerated. A more favorable model involves intervalence charge transfer.[32] The injected electrons in this model are trapped at the tungsten sites and the optical absorption is caused by resonance transfer of trapped electrons between the tungsten atoms. The third model suggests the formation of small polarons.[33,34] This theory offers a possibility to formulate a quantitative explanation for the optical absorption. Small polarons are formed when electrons polarize their surroundings, so that localization of the wavefunction takes place. A small overlap between wavefunctions corresponding to adjacent sites, as well as strong disorder is conducive to polaron formation.[34] This model uses a local structural distortion brought about by the electron trapping and W^{5+} formation. This lowers the energy of the occupied state relative to the unoccupied state of the surrounding W^{6+} . The electrochromic reaction of WO_3 is usually described by a double injection of a proton and an electron in the tungsten oxide films:

$$WO_3 + xH^+ + xe^- \leftrightarrow H_xWO_3 \qquad \text{(I.3)}$$

Despite the fact that the assumptions of this model are not verified,[3-6] the change in optical properties of the tungsten oxide films is usually attributed to the electron insertion or extraction (which means that the term xe^- is the dominating factor in equation (I.3). The data on electrochemical coloration of tungsten oxide films using the method of

cyclic voltammetry are extensively reported.[11,22,32,49-58] Gasochromic coloration of WO_3 thin films takes place by exposure of the electrochromic films to hydrogen or hydrogen containing gases in the presence of a catalyst such as Pt where some of the hydrogen gas dissociates at the catalyst into atoms.[5,6] This model of double injection to explain the coloration change has attracted a large acceptance and is comparable to the results obtained from the intervalence charge transfer theory.[32-35] According to another model proposed by George et al,[5,6] Hydrogen gas is dissociated on Platinum and transferred into pores or grain boundaries of WO_3 and subsequently creates water and an oxygen vacancy. The oxygen vacancy diffuses into the interior of the grain and water slowly desorbs from the film.[6] Studies on the formation of tungsten bronzes from the interaction of WO_3 with H_2,[62-65] H_2S,[68] NO_2,[10] SO_2[69] and NH_3,[70] gases have been carried out. For the reactions with hydrogen gas the catalyst (Pd, Pt, Rd) should be applied on the tungsten oxide surface in order to reduce the activation barrier for the reaction.[38] The coloration intensity is proportional to the partial pressure of the gas. The mechanism of gasochromic tungsten oxide reduction involves dissociation of H_2 molecules at the surface of catalyst, rapid diffusion of hydrogen to the metal/tungsten oxide interface followed by the creation of the dipole layer. This dipole layer results in a field across the interface, producing a sharp potential drop, which lowers the energy of the conduction band edge with respect to the Fermi level.[76]

The reaction of WO_3 with other gases (like H_2S or NO_2) can be described in the following way. The presence of the species in the gas phase reduces oxidized donor centers in the oxide film, which liberates electrons near the conduction band of the film. These donor centers were identified by XPS as W^{5+} sites (oxygen vacancies). The Fermi

level shift was also observed.[77] Formation of tungsten bronze upon decomposition of hydrogen-containing gases is also possible. Due to this property tungsten oxide can be used in manufacturing gas sensors. The schematic band structure explaining the optical absorption of tungsten bronze films is shown in Figure I-2. In the transparent state, the Fermi level lies between the O 2*p* and the t_{2g} bands. When tungsten oxide is reduced to bronze the Fermi level is shifted upwards and populates the lower part of the t_{2g} band with excess electrons. The material starts to exhibit absorption of visible light.

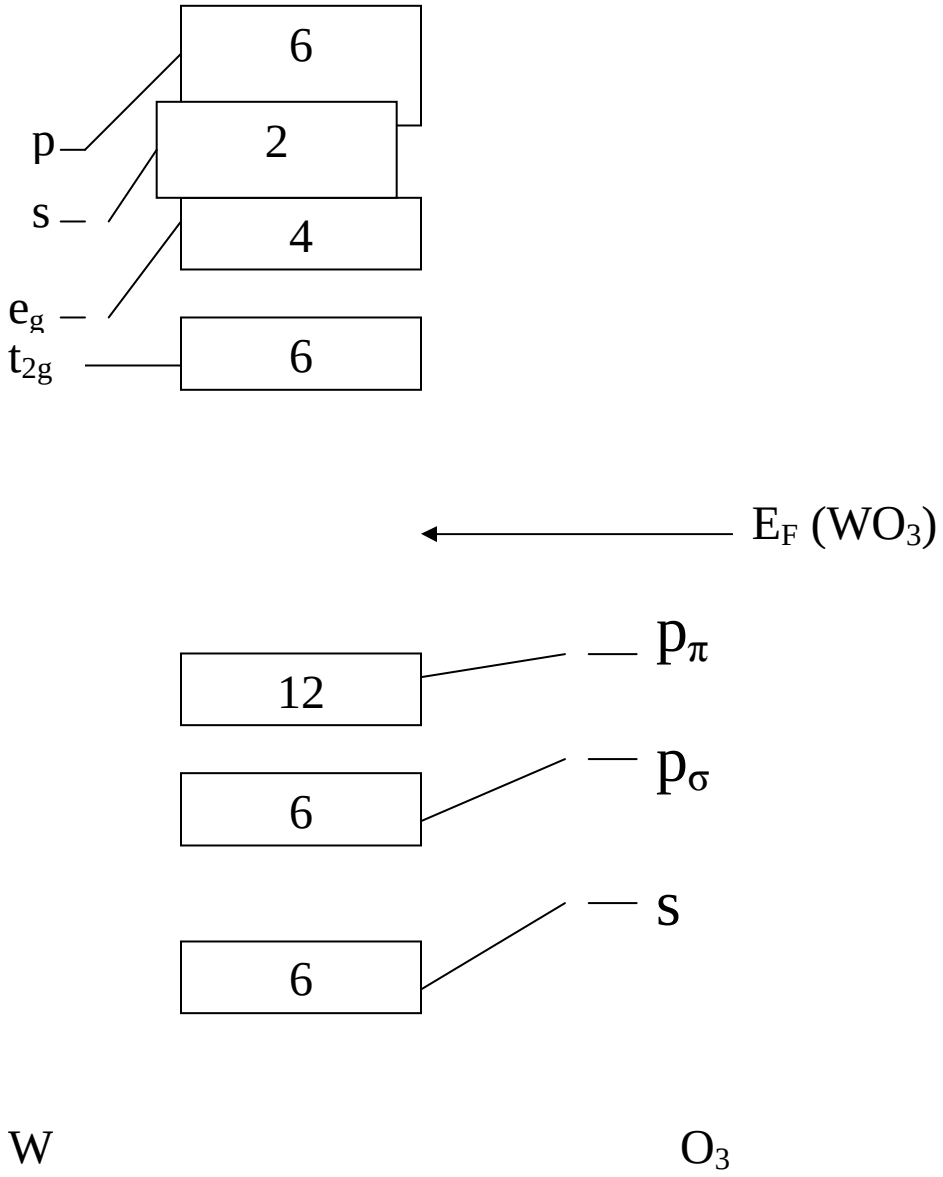

Figure I-2. Schematic band structure for WO_3 perovskite structure. Adapted from Ref. 38

C. Bleaching of hydrogen tungsten bronze

The reaction with oxygen gas normally bleaches tungsten bronzes. In this case the protons in the H_xWO_3 films are released as H_2O. When tungsten bronze is oxidized in air the rate of the oxidation is very slow and it may take several hours to decolorize the blue tungsten bronze thin film completely.[73] For the films with catalyst on the surface the process of oxidation is much faster. For example, in the case of Pt-impregnated H_xWO_3 thin films exposed to humid O_2 (20%)/ Ar mixture complete decolorization of the film takes about 20 minutes.[74]

The bleaching of tungsten bronzes can also be achieved by using other oxidizing reagents. Kikuchi *et al*. studied the kinetics of decolorization of H_xWO_3 thin films in aqueous $Fe_2(SO_4)_3$ and H_2O_2 solutions by means of UV-Vis spectroscopy.[45] The analysis of the results included solving the diffusion equations taking into account the surface reaction of the oxidizing agent with H_xWO_3. The decolorization process was found to be nearly exponential due to the non-adiabatic nature of the surface reaction between the film and the oxidizing agent. The rate-determining step is the surface reaction for a wide concentration range of the oxidizing agent. The total bleaching time for this case may lie in the region from 10 seconds to several minutes.

D. Structural properties of WO_3 and its bronzes

Tungsten trioxide crystals have perovskite-type atomic configurations ("ReO_3 type") based on corner-sharing WO_6 octahedra (Fig I-3). Deviations from the ideal cubic perovskite-type structure occur due to antiferroelectric displacements of W atoms and to mutual rotations of oxygen octahedra. Since the magnitude of distortion depends on the

temperature, at certain temperatures phase transitions may occur. There are three stable allotropic varieties of WO_3, in which the lattice is distorted to monoclinic, orthorhombic or tetragonal symmetry. The monoclinic to orthorhombic transition occurs at 330°C and the orthorhombic symmetry becomes tetragonal at 770°C. The volatility of WO_3 above 1200°C does not allow identification of a high-temperature cubic form. The overall composition can be written as WO_{3-z}, where $z>0$.[75]

At room temperature WO_3 is usually monoclinic with lattice parameters a=7.30 Å, b=7.53 Å, c=3.85 Å, β=90.88°.[77] However, if tungsten oxide hydrate ($WO_3 \cdot 2H_2O$) is annealed to 300°C it assumes a metastable cubic form, c-WO_3.[78] The relative stability of the cubic phase correlates to the presence of some kind of impurities. In another experiment with tungstic acid powder the cubic phase was observed at 200°C.[79] The initially amorphous tungsten oxide film began to crystallize after annealing to 390°C and completely adopted a crystalline phase after 450°C.[80] The crystalline structure of H_xWO_3 bronzes depends on the density of H species added to a WO_3 host. The covalent WO_3 arrays consist of WO_6 octahedra, which are distorted or regular. The W-O-W angles may vary creating a series of channels in which H atoms can be inserted. The gradual insertion of hydrogen produces an evolution of structure types similar to that caused by an increase of temperature. The distortions decrease in magnitude as the concentration of hydrogen increases. Three main phases for hydrogen tungsten bronze are found. There are reports about an orthorhombic phase at $x=0.1$,[75] whereas the tetragonal phase is formed at $x=0.23$ and $x=0.33$.[81,82] Finally, when $x \geq 0.5$ cubic tungsten bronze is obtained.[84]

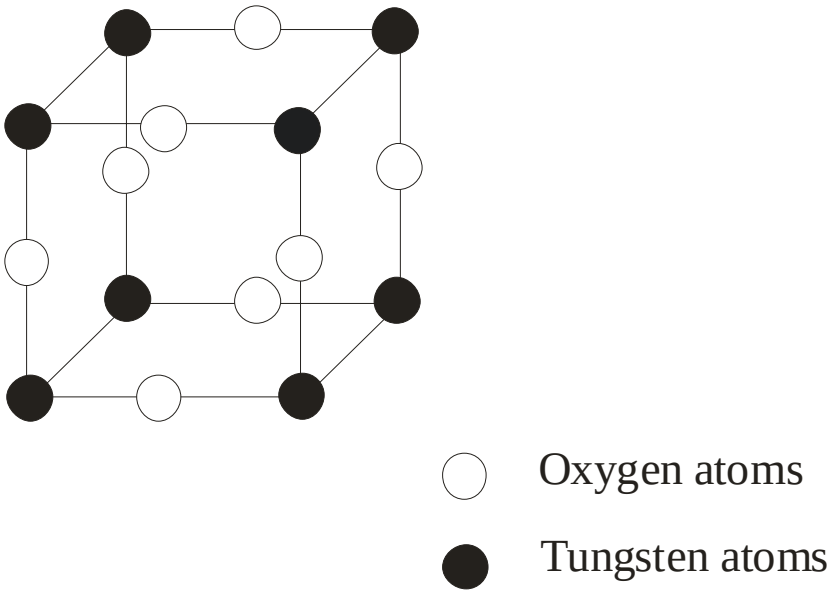

Figure I-3. The cubic "ReO_3 type" structure of WO_3. Adapted from Re

CHAPTER II

PREPARATION AND CHARACTERIZATION OF POLYCRYSTALLINE TUNGSTEN BRONZE THIN FILMS

A. Introduction

This chapter discusses the preparation and characterization of tungsten bronze thin films. The initial work in preparing these films was preformed by Evgueni B. Kadossov in Dr. Materer's group. The tungsten trioxide thin films were prepared by thermal oxidation of sputter deposited tungsten metal. These films were then reduced by Zinc under acidic conditions to give them a blue color. The structure and composition of tungsten oxide and corresponding bronzes have been determined by means of X-Ray photoelectron spectroscopy, scanning electron microscopy and ultraviolet visible spectroscopy.

B. WO_3 thin films preparation

B.1. Tungsten thin films were prepared by sputter deposition in a UHV (10^{-6} torr) chamber of metallic W (99.95% purity, A.D. Mackay, Inc.) on 2×0.6 cm quartz substrates. The deposition was carried out by ionization of argon gas and subsequent bombardment of a W target with Ar^+ ions. The ejected W species then deposit on a quartz substrate which rotates with a constant velocity. The rate of deposition was measured using a Maxtek TM-400 microbalance.

The actual thickness of W film is calculated by the following formula:

$$L(t) = \int_0^t \frac{1}{2} * F * \left|\cos(\alpha + \frac{2\pi}{T} * t')\right| dt' \qquad \text{(II.1)}$$

where F is the deposition rate (Å/s), α is the initial angle between the W species flux and the normal to the substrate, T is the period of rotation of the substrate and t is the time of deposition. The coefficient 0.5 comes from the fact that only one side of the substrate is subjected to deposition. Since t>>T, the influence of the initial angle value α on L is negligible. If the deposition rate F is constant then simplification of equation (II.1) leads to the following expression:

$$L\,(t) = 0.318 \times F \times t \qquad \text{(II.2)}$$

Thus L is linearly proportional to the time of deposition.

B.2. Oxidation of W-films

Tungsten films were converted into WO_3 films by oxidation of W in a continuous stream of oxygen at 400ºC for 3 hours according to the equation:

$$W + 3/2O_2 \rightarrow WO_3 \qquad \text{(II.3)}$$

The resulting thickness of the films was calculated regarding the difference in density between W and WO_3. From (II.3) it follows that

$$n\,(W) = n\,(WO_3) \qquad \text{(II.4)}$$

Here, n is the number of moles of a given compound per unit area. Equation (II.4) is equivalent to:

$$\frac{L(WO_3) \times \rho(WO_3)}{M(WO_3)} = \frac{L(W) \times \rho(W)}{M(W)} \qquad \text{(II.5)}$$

Where L is film thickness; ρ is density of the material and M is molecular weight of a corresponding compound. Knowing the thickness of tungsten film L (W), the thickness of the tungsten trioxide film can be calculated according to equation (II.6):

$$L(WO_3) = \frac{L(W) \times \rho(W) \times M(WO_3)}{M(W) \times \rho(WO_3)} \qquad \text{(II.6)}$$

Substituting the values for corresponding molecular weights and densities and taking into account equation (II.2) the following expression for the WO_3 film thickness is obtained:

$$L\ (WO_3) = 1.027 \times F \times t \qquad \text{(II.7)}$$

Here, F is the deposition rate from (II.1) and t is the time of deposition.

B.3. Reduction of tungsten oxide into tungsten bronze

The reduction of tungsten oxide in Zn/HCl system was done according to the procedure described in Ref. 83. WO_3 thin films were immersed into the aqueous suspension of zinc powder in which concentrated HCl acid was slowly added. The reduction of tungsten oxide to bronze was due to hydrogen evolved in the reaction:

$$Zn + 2HCl \rightarrow ZnCl_2 + H_2 \qquad \text{(II.8)}$$

The H_xWO_3 films were taken out of the reaction medium when they turned completely dark blue.

C. Characterization of WO_3 and H_xWO_3 thin films

C.1. SEM

An SEM micrograph of a WO_3 film with a thickness of 210 nm is shown in Figure II-1. The structure can be characterized as polycrystalline with island formation. The average size of a grain is estimated to be about 100 nm.

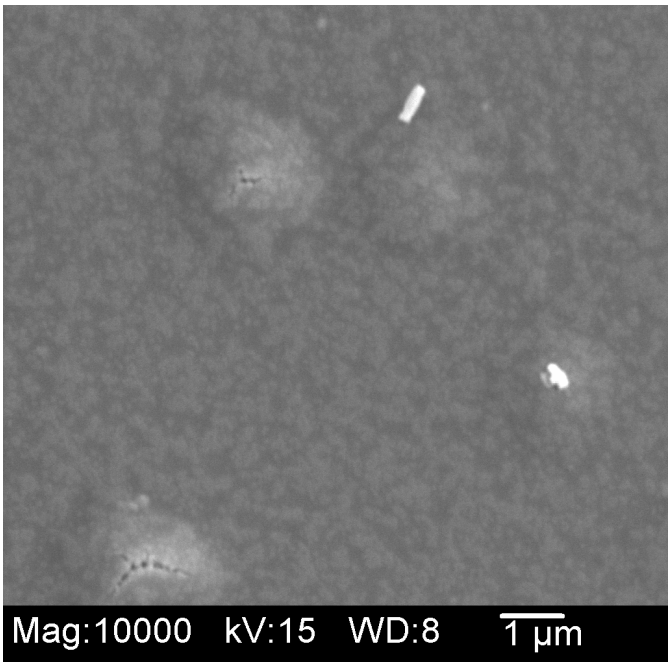

Figure II-1. SEM-micrograph of a 210 nm WO_3 film

D.2. XPS.

The XPS spectrum of a typical hydrogenated WO_3 film is shown in Figure. II-2. Three peaks attributed to W are clearly seen: a doublet W 4*d* at 261.3 eV and 246.4 eV, a broad peak at 35 eV corresponding to the splitting between $4f_{7/2}$ and $4f_{5/2}$ levels and a strong peak at 530.5 eV attributed to O 1*s*. The two peaks at 743 eV and 764 eV can be identified as oxygen KVV Auger peaks consistent with the data in Ref. 84. The spectra of H_xWO_3 thin films are practically indistinguishable from those for WO_3 in a powder form.

The deconvoluted W 4*f* peak for non-hydrogenated WO_3 is given in Figure II-3. The Gausian-Lorentzian fitting was used for the analysis. Photoelectron binding energies were calibrated with respect to C 1*s* peak centered at 284.6 eV. This peak consists of a doublet due to spin-orbit splitting between $4f_{7/2}$ and $4f_{5/2}$ levels. The separation of the doublet peaks is constant and equal to 2.15 eV. The doublet corresponding to a $4f_{7/2}$ line with binding energy 34.3 eV results from the presence of W^{6+} species in the film.[84] The XPS O 1*s* spectrum for a WO_3 film is given in Figure II-4. The main component is centered at 529.7 eV and is attributed to oxygen in the WO_3 film. Another small peak at 531.7 eV results from the presence of water bound in the film structure as well as water molecules adsorbed on the film surface.[85]

The higher binding energy constituent in the O 1*s* XPS spectrum for the H_xWO_3 film (Fig. II-5) has significantly greater intensity compared to the analogous peak for the non-hydrogenated WO_3 spectrum. This is consistent with the formation of additional O-H bonds in the process of hydrogenation. In the tungsten bronze film three doublet components in the W 4*f* deconvoluted spectrum are observed (Fig. II-6).

The first doublet with $4f_{7/2}$ at 33.6 eV corresponds to W^{6+} oxidation state analogous to that in WO_3. The second (32.9 eV) and third (30.9 eV) peaks are believed to be due to the presence of W^{5+} and W^{4+} oxidation states respectively. The relative amounts of tungsten species in hydrogenated and non-hydrogenated films are given in Table II-1.

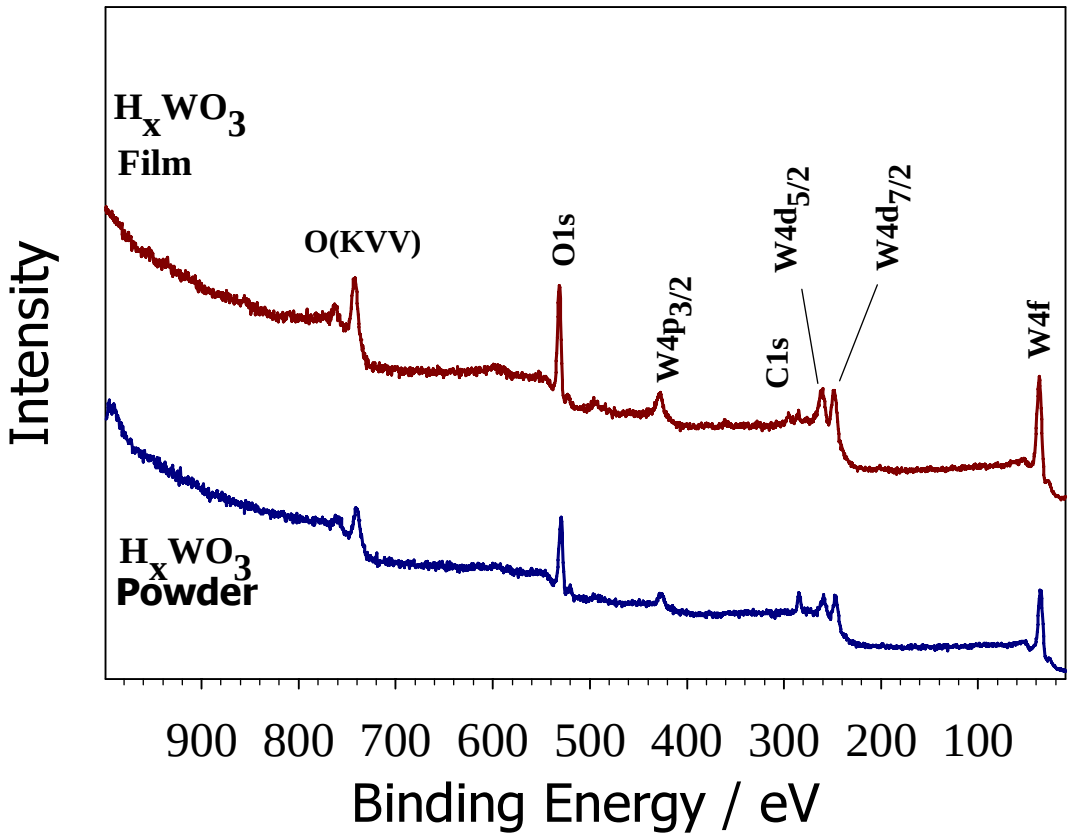

Figure II-2. XPS spectra of an H_xWO_3 thin film and H_xWO_3 in powder form.

.

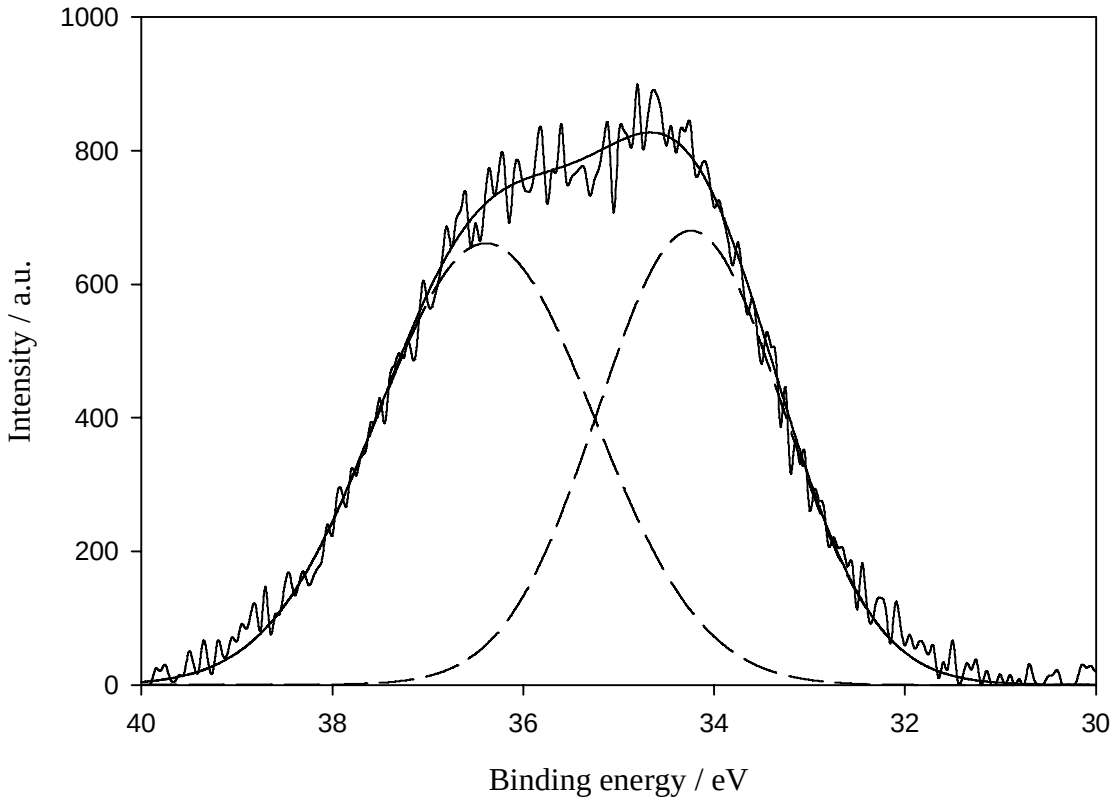

Figure II-3. XPS spectrum and deconvoluted curves for W 4*f* peak in a non-hydrogenated WO_3 film.

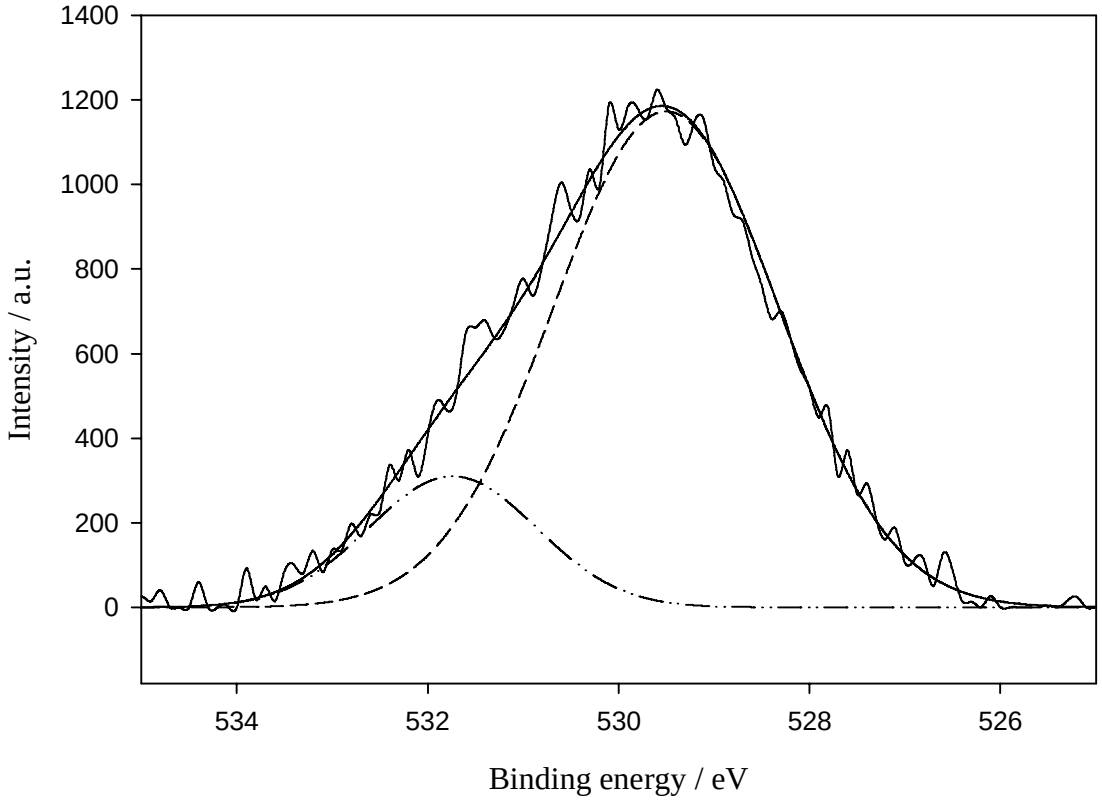

Figure II-4. XPS spectrum and deconvoluted curves for O 1*s* peak in a non-hydrogenated WO_3 film.

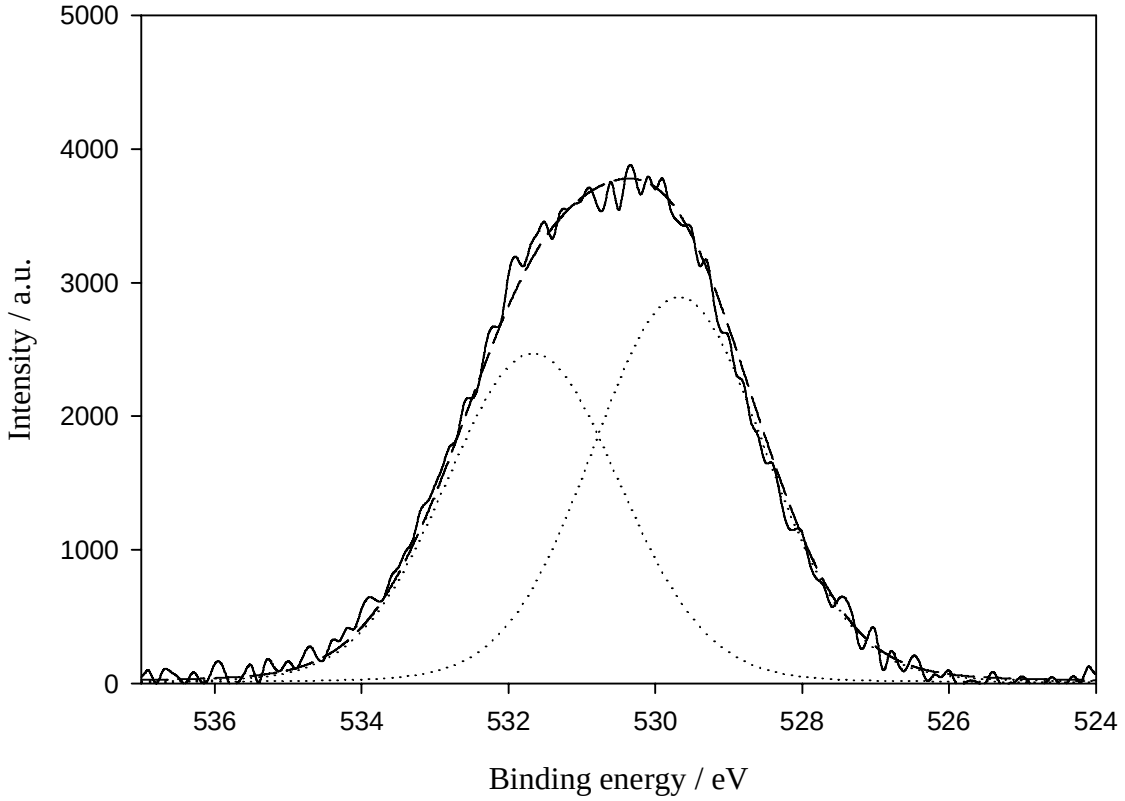

Figure II-5. XPS spectrum and deconvoluted curves for O 1*s* peak in a hydrogenated H_xWO_3 film.

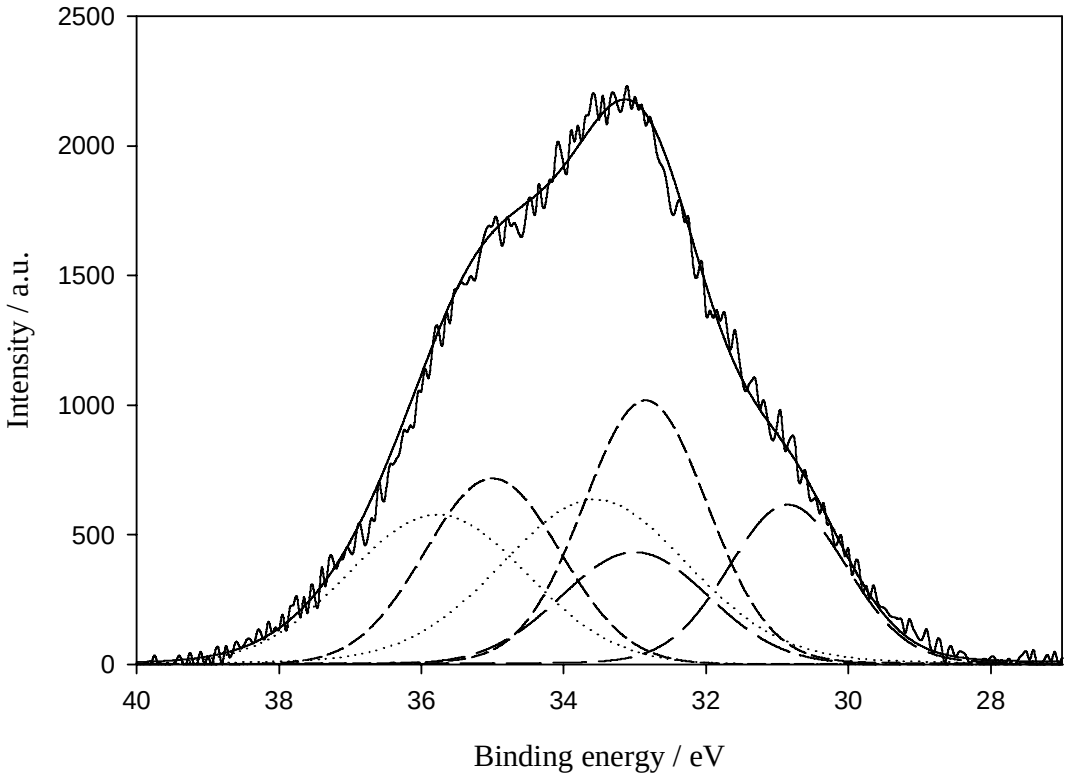

Figure II-6. XPS spectrum and deconvoluted curves for W 4*f* peak in a hydrogenated H_xWO_3 film.

	W^{6+}	W^{5+}	W^{4+}
WO_3	100	—	—
H_xWO_3	38.5	38.0	23.5

Table. II-1. Relative amounts (%) of different tungsten oxidation states in non-hydrogenated and hydrogenated WO_3 thin films.

E. Conclusions

Hydrogen tungsten bronze thin films were prepared by a two-step method. First, tungsten trioxide films were produced by sputter deposition of tungsten onto a quartz substrate with subsequent thermal oxidation in a stream of gaseous oxygen. Second, those films were reduced by a chemical reaction with hydrogen evolved in a Zn/HCl reaction medium. According to previous work done in the group, both tungsten oxide and bronzes obtained by this method possess cubic polycrystalline structure with a lattice parameter of a=3.7507 Å. This cubic structure corresponds to hydrogen tungsten bronzes with the formula H_xWO_3, where $x \geq 0.5$. While in pure tungsten oxide W^{6+} dominates, tungsten bronzes contain three types of species: W^{6+}, W^{5+} and W^{4+}. The change of optical properties in the process of WO_3 reduction is related to the shift of the Fermi level to higher energies and partial population of the lower conduction band.

CHAPTER III

OXIDATION-REDUCTION KINETICS AND DIFFUSION COEFFICIENT OF TUNGSTEN BRONZE THIN FILMS WITH NITROBENZENE

A. Introduction

Oxidation-reduction kinetics of tungsten bronze thin films and nitrobenzene were studied by ultraviolet visible spectroscopy. The concentration of nitrobenzene is held constant whereas the tungsten bronze film thickness is varied. Based upon the proposed kinetic model and the rates of the reactions for tungsten bronze thin films, the thickness dependence of the relaxation time is estimated for H_xWO_3 thin films oxidized in nitrobenzene and the diffusion coefficient of hydrogen into tungsten bronze thin films has been determined from the data. Although Evgueni B. Kadossov in Dr. Materer's group originally preformed the derivation of the diffusion equation, the experimental data presented here is new. The oxidation-reduction of tungsten bronze thin films in nitrobenzene is represented by the following equations:

$$WO_3 + X[H] \longrightarrow H_xWO_3 \qquad \text{(III.1)}$$

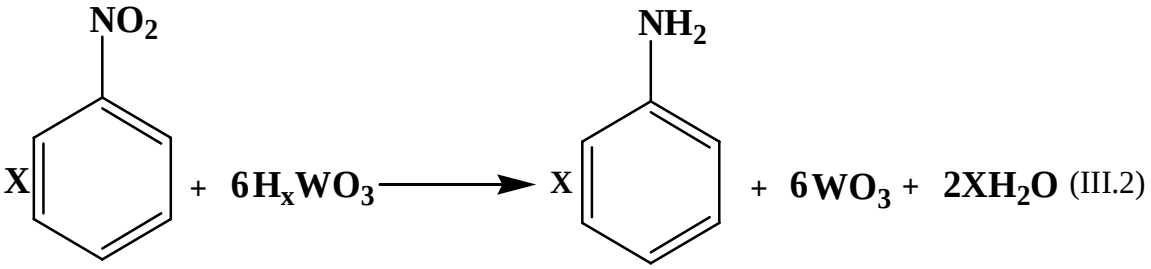

(III.2)

B. Experimental

The kinetics of oxidation of tungsten bronze films with nitro-containing organic substances was studied with a DMS-200 UV-Vis Spectrophotometer having a beam size 2×8 mm. The measurements of absorbance at a wavelength of 900 nm were taken at different time intervals. The absorbance intensity of the samples is related to the concentration *C* of hydrogen species in the film. According to Beer's law:

$$I = ALC + I_0 \tag{III.5}$$

where *A* is an absorbance coefficient, *L* is a thickness of the film and I_0 is the non-zero absorption intensity of a non-hydrogenated WO_3 sample. The intensity dependence on time for the films with different thicknesses is shown in Fig. III-1. The data are fitted quite well with the exponential relationship:

$$I = ae^{-bt} + I_0 \tag{III.6}$$

where *b* is inversely proportional to the relaxation time of the film. By fitting this expression to the experimental data the value of the reaction rate (*b)* can be obtained.

C. Kinetic model

C.1. Oxidation of tungsten bronze thin films

Since the absorbance is proportional to the total number of incorporated hydrogen atoms in the tungsten bronze film, diffusion from the bulk to the surface must be taken into account. The diffusion equation corresponding to the Fick's law looks as follows:

$$\frac{\partial C_H(x,t)}{\partial t} = D\frac{\partial^2 C_H(x,t)}{\partial x^2} \tag{III.7}$$

where $C_H(x, t)$ is the proton concentration as a function of two variables: the coordinate along the film thickness (x) and time (t); D is a diffusion coefficient. Since the reaction takes place only on one side of the film and hydrogen atoms cannot diffuse into the quartz substrate at room temperature, the first boundary condition will be:

$$\frac{\partial C_H(x,t)}{\partial x} \Big|_{x=0} = 0 \tag{III.8}$$

The second boundary condition reflects the second order reaction between the oxidant and the surface hydrogen:

$$D\frac{\partial C_H(x,t)}{\partial x} \Big|_{x=L} = kS\theta_{ox}C_H(x,t) \tag{III.9}$$

where L is the thickness of the film, k is a reaction constant, θ_{ox} is the surface coverage of the oxidizing agent, S is the total number of surface sites. The initial condition is:

$$C_H(x,t) = C_0 \text{ at } t=0 \tag{III.10}$$

Since at the very beginning of the reaction, the concentration of protons is assumed to be uniform within the film. Solving this equation for $C_H(x, t)$ *gives*:

$$C_H(x,t) = 2C_0 k' \sum_{m=1}^{\infty} \frac{\cos(\lambda_m x)}{\left[\left(k \ \lambda_m^2\right)L + k'\right]\cos(\lambda_m L)} e^{-D\lambda_m^2 t} \tag{III.11}$$

where $k' = \frac{kS\,\theta_{ox}}{D}$ and λ_m's are the roots of the equation:

$$\lambda \tan(\lambda L) - k' = 0 \tag{III.12}$$

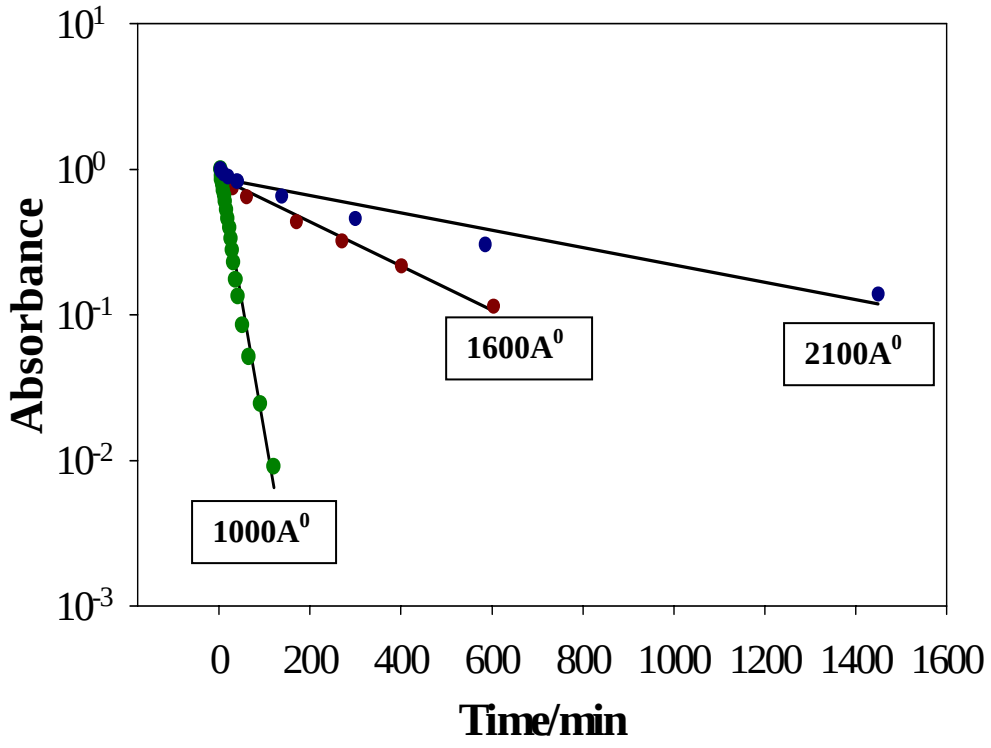

Figure III-1. Oxidation kinetics of H_xWO_3 thin films of different thickness in 3.0 M solution of nitrobenzene in ultra pure hexanes.

Fig. III-2 shows the distribution of proton concentration in a sample with thickness L changing with time. Since absorbance is proportional to $C_H(x, t)$ integrated over the thickness of the film, the time dependence of the total hydrogen concentration will be:

$$C'(t) = A\int_0^L C_H(x,t)dx = 2C_0{}'k'^2\sum_{m=1}^{\infty}\frac{1}{\lambda_m^2[(k'^2+\lambda_m^2)L+k']L}e^{-D\lambda_m^2 t} \qquad \text{(III.13)}$$

where $C_{0}{}' = A\int_0^L C_0\,dx = C_0\,LA$, A is the beam surface area.

Equation (III.13) corresponds to the exponential form of the dependence $I(t)$. The second-order equation for the change of hydrogen concentration is:

$$-\frac{dC_H}{dt} = \tilde{k}S\theta_{ox}C_H(L,t) \qquad \text{(III.14)}$$

Here, θ_{ox} is the surface coverage of nitrobenzene. Combining (III.7), (III.9) and (III.14), the relationship between the second-order reaction constant $\tilde{k}$ and the constant k from the boundary condition (III.9) will be:

$$\tilde{k}C_H(L,t) = -k\frac{dC_H}{dx}\Big|_{x=L} \qquad \text{(III.15)}$$

From equation (III.11) at $x=L$:

$$C_H(L,t) = 2C_0k'\sum_{m=1}^{\infty}\frac{1}{\left[\left(k\ \lambda_m^2\right)L+k'\right]^2}\times e^{-D\lambda_m^2 t} \qquad \text{(III.16)}$$

and

$$\frac{dC_H}{dx}\Big|_{x=L} = -2C_0k'\sum_{m=1}^{\infty}\frac{\lambda_m\tan(\lambda_m L)}{\left[\left(k\ \lambda_m^2\right)L+k'\right]^2}\times e^{-D\lambda_m^2 t} \qquad \text{(III.17)}$$

Approximating by taking just the first members of the series (III.16) and (III.17), relationship (III.15) becomes:

$$\tilde{k} = k\lambda_m \tan(\lambda_m L) \qquad \text{(III.18)}$$

Using (III.12), the equation (III.18) transforms into:

$$\tilde{k} = \frac{k^2 S\theta_{ox}}{D} \qquad \text{(III.19)}$$

The reactivity of the film can be characterized by its relaxation time $\tau=1/b$, where b is a rate constant in equation (III.6). If tan (λL) is approximated by the first two terms of the tangent series at small argument ($\tan(x) = x+x^3/3$), the dependence of τ on L can be obtained:

$$\tau = \frac{4}{\pi^2 D} L^2 + \frac{1}{kS\theta_{ox}} L \qquad \text{(III.20)}$$

Here, the relationship $1/\tau = D\lambda^2$ from equations (III.6) and (III.13) and the connection (III.12) between λ, kC_{ox} and D are used.

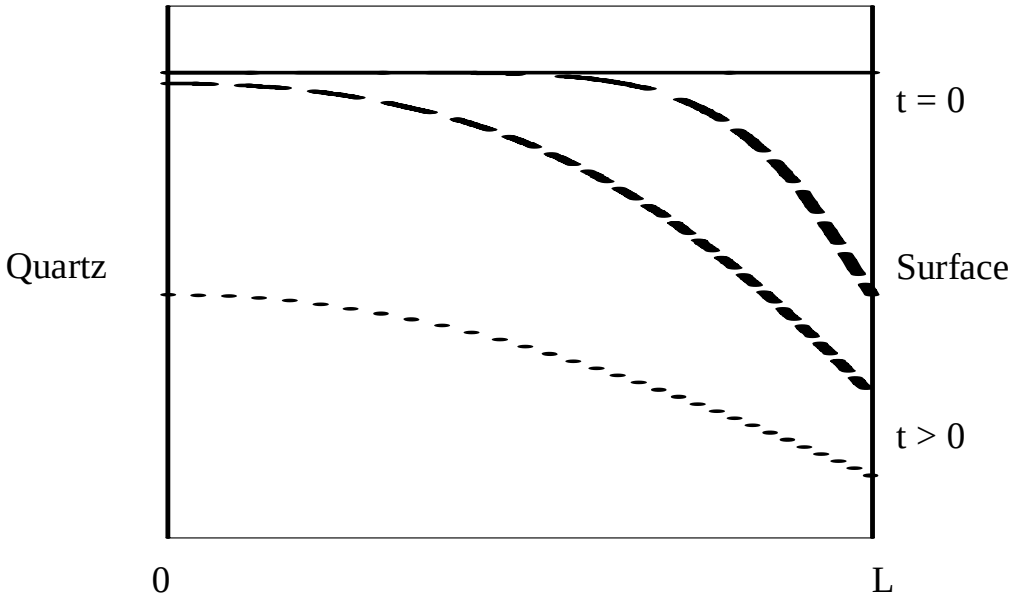

Figure III-2. Time dependent proton concentration distribution in a tungsten bronze film with thickness L.

D. Measurement of the reaction rate and diffusion coefficient of tungsten bronze thin films

A series of UV-Vis experiments studying oxidation of tungsten bronze thin films of different thicknesses in a 3.0 M solution of nitrobenzene in ultra pure hexane has been carried out. The plot showing the dependence of the relaxation time τ on the film thickness is given in Fig. III-3. It can be seen from the data that the relaxation time increases with increasing film thickness, which supports the assumption that there is a rate dependence on the diffusion of hydrogen to the surface. The plot between thickness and relaxation time gives almost a linear fit. One possible explanation for this phenomenon is that the reaction rate is much slower than the diffusion of hydrogen. Thus the linear term dominates in equation III.20. Using equation (III.16) the value of the diffusion coefficient D is estimated to be 2×10^{-13} cm^2/s, which is quite high.

E. Conclusions

The kinetics of oxidation of polycrystalline hydrogen tungsten bronze thin films involves two parameters. First, it depends on the diffusion of hydrogen from the bulk to the surface of the film. The second constituent is the reaction of surface hydrogen with the oxidizing agent. The resulting kinetic model has a linear form. This model allows estimating both the diffusion coefficient of hydrogen for the tungsten bronze films and reaction rate constant for the surface reaction. For the tungsten oxides prepared by thermal oxidation of microcrystalline W thin films, obtained by sputter deposition, the diffusion coefficient is estimated to be equal to 2×10^{-13} cm^2/s.

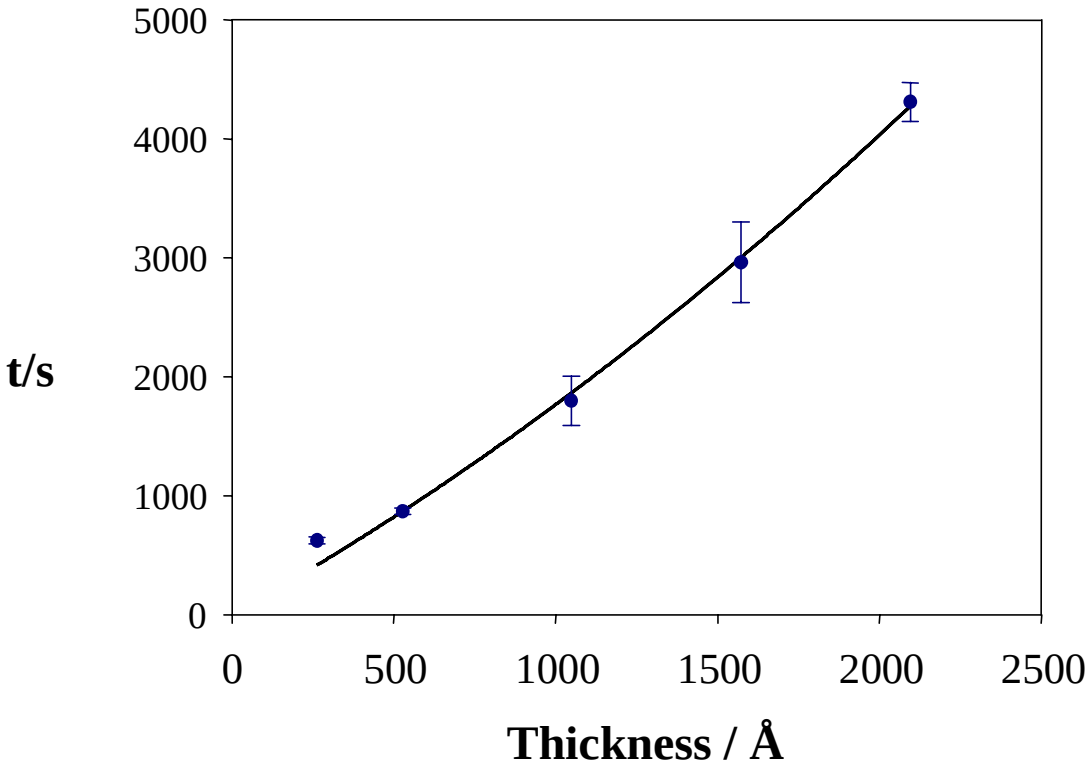

Figure III-3. Thickness dependence of the relaxation time for H_xWO_3 thin films oxidized in 3.0 M solution of nitrobenzene in ultra pure hexane.

CHAPTER IV

PREPARATION, CHARACTERIZATION AND NITROBENZENE REDUCTION KINETICS OF SILVER DEPOSITED TUNGSTEN BRONZE THIN FILMS

A. Introduction

Oxidation-reduction processes of tungsten trioxide thin films and other metal oxide surfaces with hydrogen containing gases often utilize catalysts such as platinum, palladium, gold and silver.[1-5] These catalysts increase the rate of both oxidation of H_xWO_3 to WO_3 and the rate of reduction of an oxidizing group like the nitro group to an amine. Here, the studies are done with the help of ultraviolet visible spectroscopy. Silver is deposited on WO_3 surfaces and the effect of silver concentration on the rate of reduction of nitrobenzene is studied for samples prepared by using different percentages of hydrogen in the tungsten bronze thin films. The rates of oxidation-reduction are then found while the concentration of nitrobenzene remains constant.

B. Oxidation-reduction process in the presence of a catalyst

The use of a catalyst on WO_3 surface has gained importance due to enhancement in sensitivity of the films to a particular gas[3-5]. In the presence of a catalyst the rates of

oxidation and reduction are increased dramatically as compared to the rates of reactions without a catalyst. Catalysts reduce the activation barrier for the reaction.[38] The coloration intensity is proportional to the partial pressure of the gas. The mechanism of gasochromic tungsten oxide reduction involves dissociation of H_2 molecules at the surface of catalyst, rapid diffusion of hydrogen to the metal/tungsten oxide interface followed by creation of a dipole layer. This dipole layer results in a field across the interface producing a sharp potential drop, which, in turn, lowers the energy of the conduction band edge with respect to the Fermi level.[76] Oxidation-reduction kinetics in the presence of a catalyst is explained by the following equations:

$$WO_3 + X[H] \xrightarrow[\text{Fast}]{\text{Catalyst}} H_xWO_3 \qquad \text{(IV.1)}$$

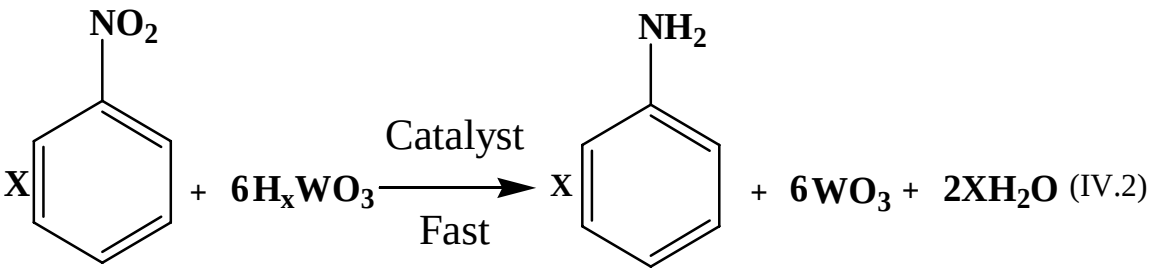

(IV.2)

C. Deposition of Silver overlayer

The effect of silver concentration on the rate of reduction of nitrobenzene is studied for samples prepared by using different percentages of hydrogen in the tungsten bronze. Silver is deposited on WO_3 films by using the reducing power of H_xWO_3, where silver replaces hydrogen of the bronze (Figure IV-1). (The use of a quartz support allows the total amount of incorporated hydrogen in the film to be quantified by monitoring the

absorbance at 900 nm while experiments using glass slides failed to produce high quality films). After preparation the films are submerged into a 0.1 M silver nitrate solution and the bronze is allowed to reduce the silver ions. This process forms a silver film on the WO_3 films. The amount of silver is controlled by using films with different hydrogen concentrations and quantified by the percent decrease in the absorbance of the films at 900 nm with respect to that of freshly prepared samples. This process involves, reducing the WO_3 films using zinc metal in an acidic (HCI) solution, allowing the films to oxidize in air until the absorbance is 0%, 15%, 25%, 50%, 75% and 100% of the respective initial absorbance and then submerging them into the silver nitrate solution.

$$H_xWO_3 + Ag^+ \longrightarrow Ag.WO_3 + X\,H^+ \qquad \text{(IV.3)}$$

D. Characterization of silver deposited WO_3 and H_xWO_3 thin films

D.1. SEM and XPS.

SEM micrographs of 105 nm thick silver coated WO_3 films under optimal conditions are shown in Figure IV-2. Under optimal conditions the silver particles are evenly distributed over the film. This may be the reason for fast transfer of hydrogen into and out of the thin films as compared to the non-optimal conditions.

The XPS spectrum of a silver coated WO_3 film is shown in Figure IV-3. Two additional peaks, Ag $3d_{5/2}$ at 368.3 eV and Ag $3d_{3/2}$ at 375.5 eV, can clearly be seen in the spectrum of these films which proves the presence of silver on the WO_3 film.

E. Reaction rates of silver deposited WO_3 thin Films with nitrobenzene

Once formed, the oxidation kinetics of the tungsten bronze films and the concomitant reduction of nitrobenzene are studied by measuring the absorption of 900 nm light as a function of time. The rate of reduction of 3.0 M nitrobenzene solution in ultrapure hexane is studied for samples prepared by using different percentages of hydrogen in the tungsten bronze. Figure IV-4 shows the nitrobenzene reaction rates with tungsten bronze thin films, which are produced from 0%, 15%, 25%, 50%, 75% and 100% hydrogen in the films. The rate of reaction for a blank sample, without silver is found to be 0.03 min^{-1}, while the rates of reaction of samples made by using different percentages of hydrogen in the samples is observed to be enhanced by the silver catalyst. The fastest reduction rate of nitrobenzene is obtained from silver coated tungsten bronze films prepared from bronze film whose absorbance at 900 nm has decayed to 75%-100% of its initial value. SEM and XPS studies of these films show that the even distribution of silver particles on the surface is responsible for the increased oxidation and reduction rates.

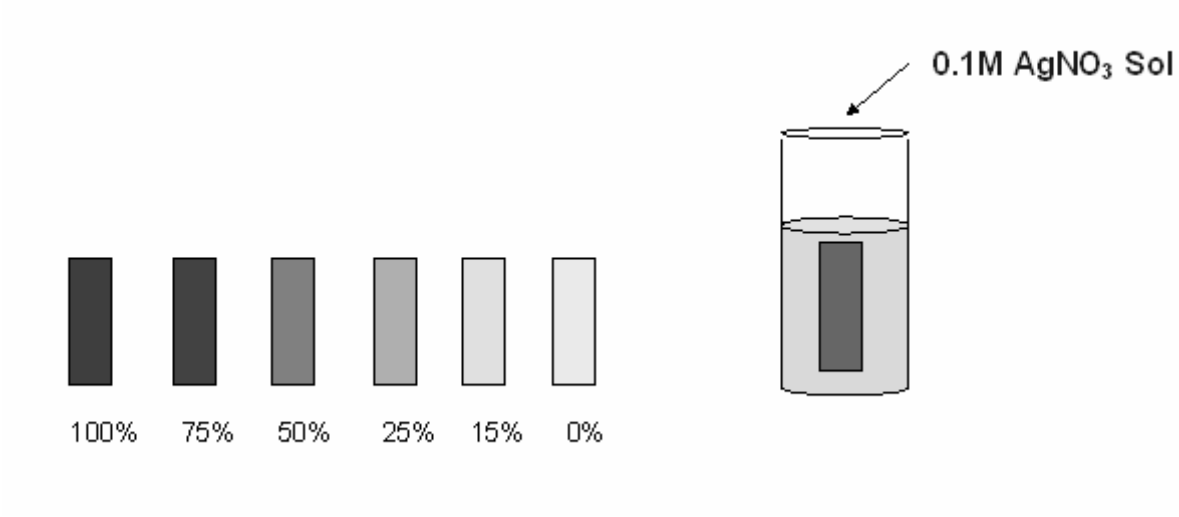

Figure IV-1. Control of deposition of silver by using the different percentages of hydrogen in the tungsten bronze.

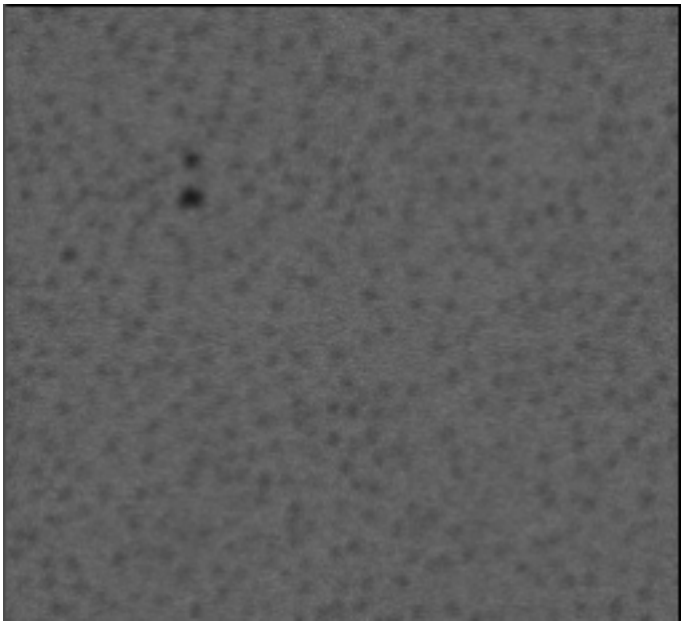

Figure IV-2. SEM-micrograph of a 105 nm Silver deposited WO_3 film under optimized conditions. A beam energy of 5 keV and a magnification of 1300 has used.

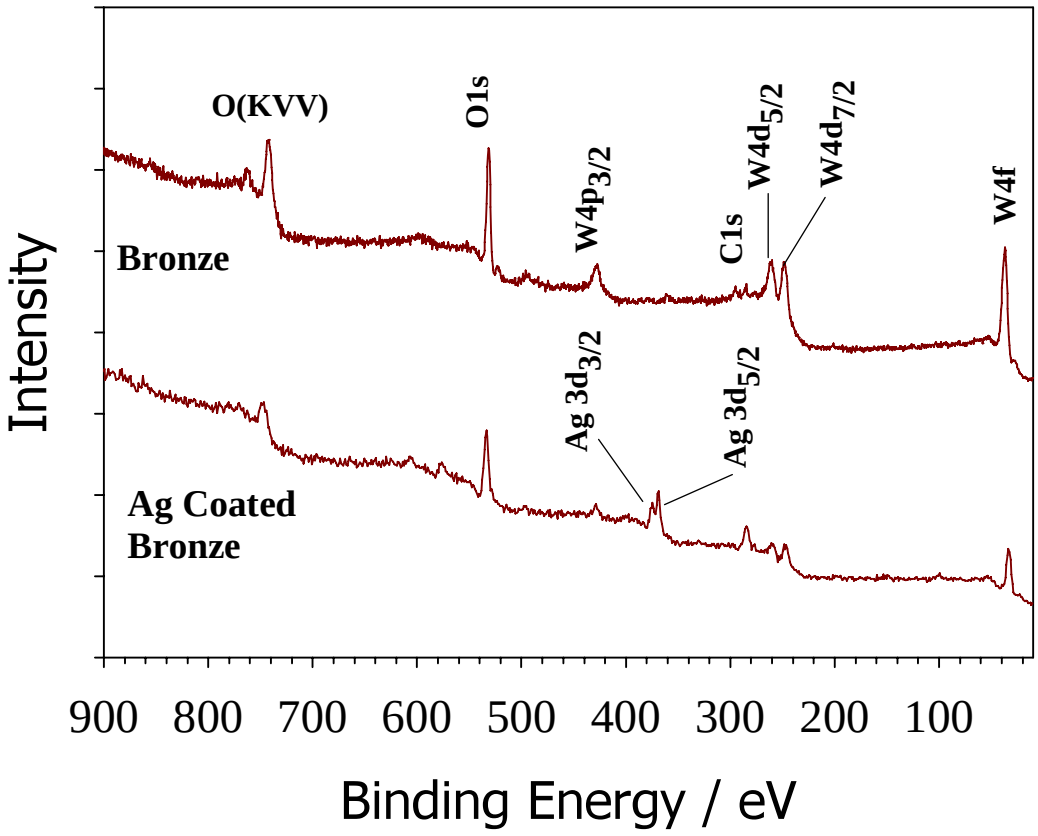

Figure IV-3. XPS spectra of an H_xWO_3 thin film and Ag coated H_xWO_3

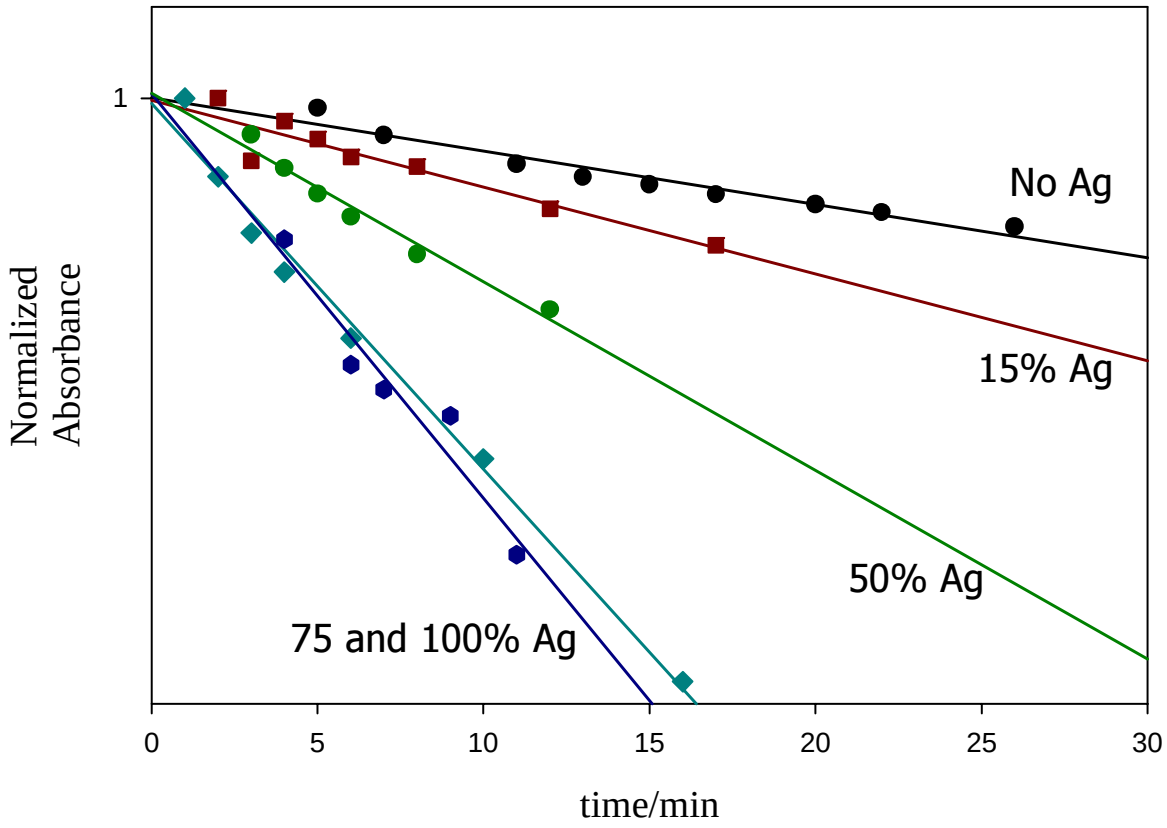

Figure IV-4. The rates of reduction of nitrobenzene for samples prepared by using different percentages of hydrogen in the tungsten bronze.

CHAPTER V

FIRST ROW TRANSITION METAL CATALYZED REACTIONS OF TUNGSTEN BRONZE THIN FILMS WITH NITROBENZENE

A. Introduction

After finding the optimal percentage of hydrogen in the tungsten bronze thin films for silver deposition, these conditions are used further for the deposition of first row transition metals titanium (Ti), chromium (Cr), manganese (Mn), iron (Fe), cobalt (Co), nickel (Ni) and copper (Cu) on tungsten trioxide films surfaces. The increase in reaction rate of these films with 3.0 M nitrobenzene is studied by monitoring the ultraviolet visible absorbance at 900 nm while keeping the concentration of nitrobenzene constant.

B. Deposition of first row transition metals on WO_3 thin films and reaction rate determination with nitrobenzene

First row transition metals are deposited on tungsten bronze surfaces by using 0.1 M solutions of Ti, Cr, Mn, Fe, Co, Ni and Cu ions. The 1048 nm bronze films are freshly prepared before submerging the films into these solutions for approximately 12 hours. After depositing, the coated films are converted to bronzes using Zn/HCl. Once the bronze has been formed, the reaction rate with 3 M nitrobenzene is determined.

B.1. Deposition of titanium

Titanium is deposited on WO_3 films by leaving the films over night in a 0.1 M

solution of titanium chloride (MW 128.5) in HCl. The solution is first diluted in a 100 ml measuring flask by taking 8.3 ml of concentrated titanium chloride solution, adding about 10ml of 1 M NaOH solution and then hydrogen peroxide and water until the excess HCl is neutralized. The rate of reaction for these films with 3.0 M nitrobenzene is then determined. The rate of reaction of titanium-coated films is as much as 4.31 times faster than the films with out the titanium over layer.

B.2. Deposition of chromium

Chromium is deposited on WO_3 films by submerging the films over night in a 0.1 M solution of chromium III acetate, basic ($C_{14}H_{23}Cr_3O_{16}$ MW 603.32). The solution is made by dissolving 6.032 grams chromium III acetate, basic and water in a 100ml-measuring flask. The rate of reaction for these films with 3.0 M nitrobenzene is then determined. The rate of reaction of chromium-coated films is about 1.42 times faster as compared to the films without chromium catalyst.

B.3. Deposition of manganese

Manganese is deposited on WO_3 films by submerging the films over night in a 0.1 M solution of manganese chloride ($MnCl_2.2H_2O$, MW 198). The solution is made by dissolving 1.98 grams manganese chloride in water in a 100 ml measuring flask. The rate of reaction for these films with 3.0 M nitrobenzene is then determined. The rate of reaction of chromium-coated films is about 2.81 times faster as compared to the films without manganese catalyst.

B.4. Deposition of iron

Iron is deposited on WO_3 films by leaving the films over night in a 0.1 M solution of ferrous sulphate ($FeSO_4.7H_2O$, MW 278). To make a 0.1 M solution of the salt, 2.78 grams of ferrous sulphate are dissolved in water in a100 ml measuring flask. The rate of reaction for these films with 3.0 M nitrobenzene is then determined. The rate of reaction of iron-coated films is about 4.03 times faster than that of films without the iron over layer.

B.5. Deposition of cobalt

Cobalt is deposited on WO_3 films by submerging the films over night in a 0.1 M solution of cobalt oxalate ($CoC_2O_4.2H_2O$, MW 183). The solution is made by taking 1.83 grams cobalt acetate and water in a 100 ml measuring flask. The rate of reaction for these films with 3.0 M nitrobenzene is then determined. The rate of reaction of cobalt-coated films is about 3.81 times faster as compared to the films without cobalt catalyst.

B.6. Deposition of nickel

Nickel is deposited on WO_3 films by submerging the films over night in a 0.1 M solution of Nickel chloride ($NiCl_2.6H_20$ MW 237.7). The solution is made by taking 2.377 grams Nickel chloride and water in a 100 ml measuring flask. The rate of reaction for these films with 3.0 M nitrobenzene is then determined. The rate of reaction of Nickel coated films is about 2.74 times faster as compared to the films without Nickel catalyst.

B.7. Deposition of copper

Copper is deposited on WO_3 films by leaving the films over night in a 0.1 M solution of copper sulphate ($CuSO_4.5H_2O$, MW 249.5). To make a 0.1 M solution of the salt 2.495 grams of copper sulphate are dissolved in water in a 100ml measuring flask. The rate of reaction for these films with 3.0 M nitrobenzene is then determined. The rate of reaction of copper coated films is about 3.37 times faster than that of films without the copper over layer.

The trend in the first row of transition metals for rates of reaction and their ratios to the rates of reaction for blank WO_3 films is shown in table V-1. A quick increase in rate of reaction is found for Ti and then the rates with other metals form a volcano shape curve as the atomic number increases.

	A	B	C	D	E	F
52	**Element**	**At No**	**Sample No**	**Rates**	**Avg Rates**	**Rate ratio**
53						
54	**Ti**	**22**	**1**	**0.121**	**0.129**	**4.31**
55			**2**	**0.133**		
56			**3**	**0.133**		
57						
58	**Cr**	**24**	**1**	**0.039**	**0.043**	**1.42**
59			**2**	**0.041**		
60			**3**	**0.049**		
61						
62	**Mn**	**25**	**1**	**0.082**	**0.085**	**2.81**
63			**2**	**0.08**		
64			**3**	**0.092**		
65						
66	**Fe**	**26**	**1**	**0.121**	**0.121**	**4.03**
67			**2**			
68			**3**	**0.121**		
69						
70	**Co**	**27**	**1**	**0.128**	**0.114**	**3.81**
71			**2**	**0.111**		
72			**3**	**0.102**		
73						
74	**Ni**	**28**	**1**	**0.072**	**0.082**	**2.74**
75			**2**	**0.067**		
76			**3**	**0.108**		
77						
78	**Cu**	**29**	**1**	**0.096**	**0.101**	**3.37**
79			**2**	**0.111**		
80			**3**	**0.096**		
81						
82	**Ag**	**47**	**1**	**0.071**	**0.061**	**2.04**
83			**2**	**0.062**		
84			**3**	**0.051**		

Table V-1. Rates of reactions of WO_3 films with metal over layer

CHAPTER VI

CONCLUDING REMARKS

Hydrogen tungsten bronze thin films were prepared in two steps. First, sputtered tungsten thin films were thermally oxidized in a stream of oxygen gas at 400°C. Second, the resulting tungsten oxide films were reduced to bronze by using zinc metal in an acidic solution. The films were characterized by means of Scanning Electron Microscopy and X-Ray Photoelectron Spectroscopy. Both tungsten oxide and tungsten bronze display cubic polycrystalline structure, which is typical for tungsten bronzes with high hydrogen content. X-Ray Photoelectron Spectroscopy and visible spectroscopic results performed previously, confirm that these films are indistinguishable by composition from conventionally prepared tungsten bronze powders. Once formed, the reduction kinetics of nitrobenzene and the concomitant oxidation of the tungsten bronze films are studied by measuring the ultraviolet visible absorbance at 900 nm as a function of time. Combination of these two parameters results in a complex model with the exponential time dependence of total hydrogen concentration in the film. Proper fitting of the experimental data allows estimation of the hydrogen diffusion coefficient of hydrogen in tungsten bronze films. The value of the diffusion coefficient is estimated to be equal to 2×10^{-13} cm^2/s. To increase the surface reaction rate, various transition metals (Ag, Ti, Cr, Mn, Fe, Co, Ni and Cu) are deposited on the surface using wet chemistry.

For silver deposited films the amount of silver is controlled by using films with different hydrogen concentrations and quantified by the percent decrease in the absorbance of the films at 900 nm with respect to the absorbance of the freshly prepared samples. The fastest reduction rate of nitrobenzene is obtained from silver coated tungsten bronze films prepared from an uncoated bronze film whose ultraviolet visible absorbance at 900 nm decays to 75%-100% of its initial absorbance. The rate of oxidation of films with nitrobenzene is studied to find an optimum hydrogen concentration in the films. From kinetic data an enhanced rate of reaction is found due to the catalytic activity of silver on tungsten bronze thin films. SEM and XPS studies of these films show that the even distribution of silver particles on the surface is responsible for the fast oxidation of tungsten bronze thin films and the concomitant reduction of nitrobenzene.

In addition to silver, 1^{st} row transition metals coated bonze films are also prepared. In general, the reaction rate increases with atomic number toward a maximum around iron and then decreases forming a volcano shaped curve. One exception to this general trend is the titanium coated bronze film. The reaction rate of titanium-coated films exceeds that of all other transitions metals studied.

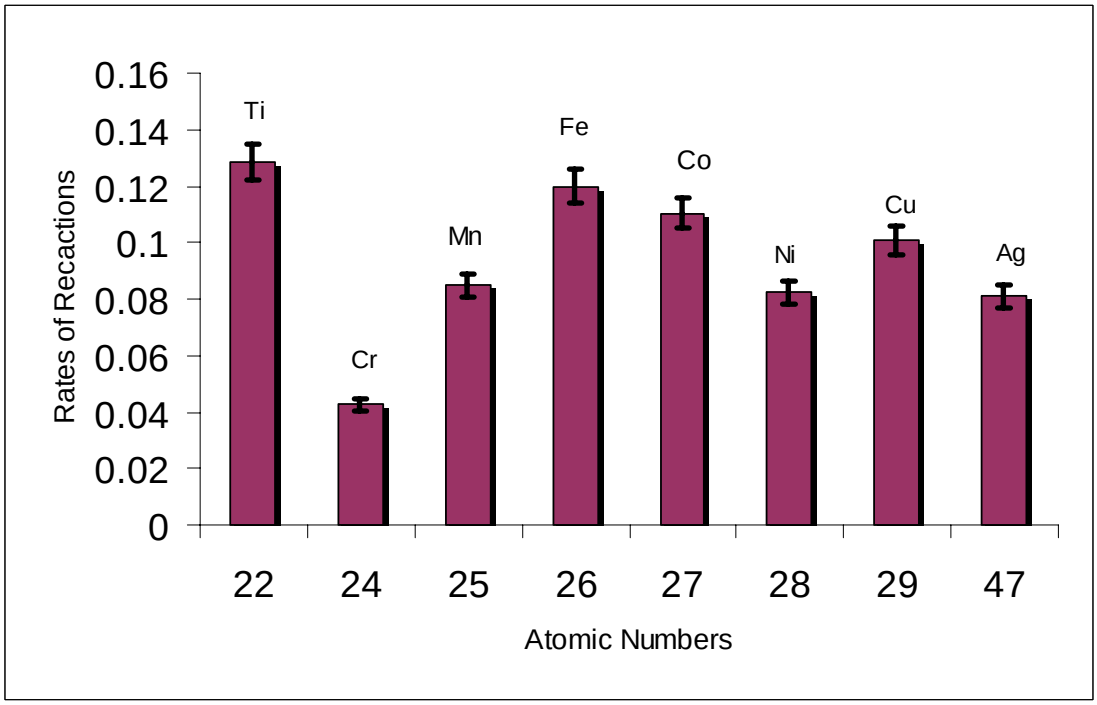

Figure VI-1. Increase in the rates of reactions of WO_3 films with metal over layer

BIBLIOGRAPHY

1. Apblett, A.W., Kiran, B.P., Malka, S.; Materer, N.F. and Piquette, A., *Ceramic Transactions* 2006, *172*, 29
2. Apblett, A.W., Kiran, B.P., and Oden, K., *ACS Symposium Series* 2003, *837*, 154.
3. Vraghuveer, B. Viswanathan, *J of Power Sources* 2005, *144*, 1
4. Ippolito, S.J., Kandasamy, S., Kalantar-zadeh, K. and Wlodarski, W., *Sensors and Actuators B.* 2005, *108*, 553
5. Wgraf, G., Neumann, R., Witter, V., *Solar Energy Materials & Solar Cells* 2000, *63*, 165.
6. Shanak, H., Schmitt, H., Nowoczin, J. and Ziebert, C., *Solid State Ionics,* Volume 171, Issue 1-2, 30 June 2004, 99-106
7. Bartha, L. and Kiss, A.B., *Int. J. of Refractory Metals & Hard Materials* 1995, *13*, 77
8. Sum, H.-T., Cantalini, C., Lozz, L., Passacantando, M., Santucci, S., and Delino, M., *Thin Solid Films* 1996, *287*, 258.
9. Sberveglieri, G., Depero, L., Groppelli, S., and Nelli, P., *Sensors and Actuators B* 1995, *26-27*, 89.
10. Wang, S.-H., Chou, T.-C., and Liu, C.-C., *Sensors and Actuators B* 2003, *94*, 343.
11. Lampert, C.M., *Sol. Energy Mater.* 1984, *11*, 1.
12. Svenson, J. and Granqvist, C., *Appl. Phys. Lett.* 1984, *45*, 828.

13. Faughnan, B.W. and Crandall, R.S., in *Topics in Applied Physics*, J. Pankov, Editor. 1980, Springer: Berlin.

14. Agniohotry, S.A., Saini, K.K., and Chandra, S., *Indian J. Pure Appl. Phys.* 1986, *24*, 19. Baucke, F.G.K., *Sol. Energy Mater.* 1987, *16*, 67.

15. Deneuville, A. and Gerard, P., *J. Electron. Mater.* 1978, *7*, 559. Mucke, K., Bohm, F., Gambke, T., Ottermann, C., and Bange, K., *SPIE* 1990, *1323*,

16. Hichwa, B.P., Caskey, G., Betz, D.F., and Harlow, J.D., *J. Vac. Sci. Technol.* 1987, *5*, 1775.

17. Davazoglou, D., Donnadieu, A., Fourcade, R., Hugot-le Goff, A., Delichere, P., and Perez, A., *Rev. Phys. Appl.* 1988, *23*, 265.

18. Davazoglou, D., Leveque, G., and Donnadieu, A., *Sol. Energy Mater.* 1988, *17*, 379.

19. Tracy, C.E. and Benson, D.K., *J. Vac. Sci. Technol. A* 1986, *4*, 2377.

20. Delichere, P., Falaras, P., Froment, M., Hugot-le Goff, A., and Agius, B., *Thin Solid Films* 1988, *161*, 35.

21. Ohtsuka, T., Goto, N., and Sato, N., *J. Electroanal. Chem.* 1990, *287*, 249.

22. Unuma, H., Tonooka, K., Suzuki, Y., Furusaki, T., Kodaira, K., and Matsushita, T., *J. Mater. Sci. Lett.* 1986, *5*, 1248

23. Yamanaka, K., Oakamoto, H., Kidou, H., and Kudo, T., *Jpn. J. Appl. Phys.* 1986, *25*, 1420.

24. Habib, M.A., Maheswari, S.P., and Carpenter, M.K., *J. Appl. Electrochem.* 1991, *21*, 203.

25. Baba, N. and Yohino, T., *J. Appl. Electrochem.* 1982, *12*, 607.

26. Miles, M.H., Stilwell, D.E., Hollins, R.A., and Henry, R.A., in *Electrochromic Materials,* M.K. Carpenter and D.A. Corrigan, Editors. 1990,
27. The Electrochemical Society: Pennington. p. 137. Wertheim, G.K., Campagna, M., Chazalviel, J.-N., Buchanan, D.N.E., and Shanks, H.R., *Appl. Phys.* 1977, *13*, 225.
28. Gerand, G., Nowogrocki, G., Guenot, J., and Figlarz, M., *J. Solid State Chem.* 1979, *29*, 429.
29. Deb, S.K., *Appl. Opt. (Suppl.3)* 1969, 192.
30. Crandall, R.S. and Faughnan, B.W., *Appl. Phys. Lett.* 1976, *28*, 95.
31. Wittwer, V., Schirmer, O.F., and Schlotter, P., *Solid State Commun.* 1978, *25*, 977.
32. Kukuev, V.I., Tutov, E.A., Domashevskaya, E.P., Yanovskaya, M.I., Obvintseva, I.E., and Venevtsev, Y.N., *Soviet Phys. Tech. Phys.* 1987, *32*, 1176.
33. Niehus, H., *Surf. Sci.* 1978, *78*, 667.
34. Bange, K., *Sol. Energy Mater.* 1999, *58*, 1.
35. Goulding, M.R., Thomas, C.B., and Hurditch, R.J., *Solid State Commun.* 1983, *46*, 451.
36. Shigesato, Y., *Jpn. J. Appl. Phys.* 1991, *30*, 1457.
37. Kukuev, V.I., Komolova, L.F., Lesovoy, M.V., and Tomaspolsky, Y.Y., *J. Microsc. Spectrosc. Electron.* 1989, *14*, 471.
38. Gerard, P., Deneuville, A., and Courths, R., *Thin Solid Films* 1980, *71*, 221.
39. Bechinger, C., Herminghaus, S., and Leiderer, P., *Thin Solid Films* 1994, *239*, 156.

40. Bechinger, C., Oetinger, G., Herminghaus, S., and Leiderer, P., *J. Appl. Phys.* 1993, *74*, 4527. Kikuchi, E., Hirota, N., Fujishima, A., Itoh, K., and Marabayashi, M., *J. Electroanal. Chem.* 1995, *381*, 15.
41. Garrilynk, A.I., Zakarchenya, B.P., and Chudnovskii, F.A., *Sov. Tech. Phys. Lett.* 1980, *6*, 512.
42. Garrilynk, A.I., Lanskaya, T.G., and Chudnovskii, F.A., *Sov. Tech. Phys. Lett.* 1987, *32*, 964.
43. Nagasu, M. and Koshida, N., *Appl. Phys. Lett.* 1990, *57*, 1324.
44. Kikuchi, E., Iida, K., and Fujishima, A., *J. Electroanal. Chem.* 1993, *351*, 105.
45. Yao, J.N., Loo, B.H., and Fujishima, A., *Ber. Bunsenges. Phys. Chem.* 1990, *94*, 13.
46. Bange, K., Martens, U., Nemetz, A., and Temmink, A., in *Electrochromic Materials, Proc.*, M.K. Carpenter and D.A. Corrigan, Editors. 1990, The Electrochemical Society: Pennington, USA. p. 334.
47. Delichere, P., Falaras, P., and Hugot-le Goff, A., *Sol. Energy Mater.* 1989, *19*, 323.
48. Dautremont-Smith, W.C., *Displays* 1982, *3*, 67.
49. Chang, I.F., Gilbert, B.L., and Sun, T.I., *J. Electrochem. Soc.* 1975, *122*, 955.
50. Dickens, P.G. and Whittingham, M.S., *Q. Rev. Chem. Soc.* 1968, *22*, 30.
51. Green, M., Smith, W.C., and Weiner, J.A., *Thin Solid Films* 1976, *38*, 89.
52. Hersh, N.H., Kramer, W.E., and McGee, J.H., *Appl. Phys. Lett.* 1975, *27*, 646.
53. Green, M. and K.S., K., *Thin Solid Films* 1977, *40*, L19.
54. Patil, P.R., Pawar, S.H., and Patil, P.S., *Solid State Ionics* 2000, *136-137*, 505.

55. Yao, J.N., Chen, P., and Fujishima, A., *J. Electroanal. Chem.* 1996, *406*, 223.

56. Vertes, A. and Schiller, R., *J. Appl. Phys.* 1983, *54*, 199.

57. Vertes, A. and Schiller, R., *Studies in Inorganic Chemistry* 1982, *3*, 299

58. Kamimory, T., Nagai, J., and Mizuhashi, M., *Proc. SPIE* 1983, *428*, 51.

59. Hitchman, M., *Thin Solid Films* 1979, *61*, 341.

60. Rauh, R.D., *Solid State Ionics* 1988, *28-30*, 1479.

61. Schweiger, D., Georg, A., Graf, W., and Witter, V., *Sol. Energy Mater. & Solar Cells* 1998, *54*, 99.

62. Zhuang, L., Xu, X., and Shen, H., *Surf. Coatings Tech.* 2003, *167*, 217.

63. Fruhberger, B., Grunze, M., and Dwyer, D.J., *Sensors and Actuators B* 1996, *31*, 167.

64. Penza, M., Cassano, G., and Tortorella, F., *Sensors and Actuators B* 2001, *81*, 115.

65. Meixner, H., Gerblinger, J., Lampe, U., and Fleischer, M., *Sensors and Actuators B* 1995, *23*, 119.

66. Rye, R.R. and Ricco, A.J., *J. Appl. Phys.* 1987, *62*, 1084.

67. Dwyer, D.J., *Sensors and Actuators B* 1991, *5*, 155.

68. Nishimura, N., Aikawa, Y., and Sukigara, M., *Nippon Shashin Gakkaishi* 1985, *48*(6), 421.

69. Opara-Krasovec, U., Jese, R., Orel, B., Grdadolnik, J., and Drazic, G., *Monatshefte fur Chemie* 2002, *133*, 1115.

70. Kim, D.-J. and Pyun, S.-I., *J. Corros. Sci. Soc. of Korea* 1996, *27*(4), 442.

71. Bringans, R.D., Hochst, H., and Shanks, H.R., *Phys. Rev. B* 1981, *24*(6), 3481.

72. Salje, E. and Viswanathan, K., *Acta. Crystallogr. Sec. A* 1975, *31*, 356.

73. Balazsi, C., Farkas-Jahnke, M., Kotsis, I., Petras, L., and Pfeifer, J., *Solid State Ionics* 2001, *141-142*, 411.

74. Perry, W.L., Smith, B.L., Bullian, C.J., Busse, J.R., Macomber, C.S., Dye, R.C., and Son, S.F., *Propellants, Explosives, Pyrotechnics* 2004, *29*(2), 99.

75. Ozkan, E., Lee, S.-H., Tracy, C.E., Pitts, J.R., and Deb, S.K., *Sol. Energy Mater.* 2003, *79*, 439.

76. Dickens, P.G. and Hurditch, R.J., *Nature* 1967, *215*, 1266.

77. Agnihotry, S.A., Rashmi, Ramchandran, R., and Chandra, S., *Sol. Energy Mater.* 1995, *36*, 289.

78. Ayyappan, S. and Rao, C.N.R., *Mater. Res. Bull.* 1995, *30*(8), 947.

79. Sienko, M.J. and Oesterreicher, H., *J. Am. Chem. Soc.* 1968, *90*(23), 6568.

80. Barreca, D., Carta, G., Rossetto, G., Tondello, E., and Zanella, P., *Surf. Sci. Spectra* 2001, *8*(4), 258.

81. Leftheriotis, G., Papaefthimiou, S., and Siokou, A., *Thin Solid Films* 2001, *384*, 298.

82. Bringans, R.D., Hochst, H., and Shanks, H.R., *Surf. Sci.* 1981, *111*, 80.

83. Hochst, H. and Bringans, R.D., *Appl. Surf. Sci.* 1982, *11/12*, 768

84. Bringans, R.D., Hochst, H., and Shanks, H.R., *Vacuum* 1981, *31*(10-12), 473.

85. Tritthart, U., Gey, W., and Gavrilyuk, A., *Ionics* 1998, *4*, 299.

86. Loo, B.H., Yao, J.N., Coble, H.D., Hashimoto, K., and Fujishima, A., *Appl. Surf. Sci.* 1994, *81*, 175.

87. Vannice, M.A., Boudart, M., and Fripiat, J.J., *Journal of Catalysis* 1970, *17*, 359

VITA

Kashif Rashid Khan

Candidate for the Degree of

Masters of Science

Thesis: PREPARATION AND NITROBENZENE REACTION KINETICS OF MICROCRYSTALLINE TUNGSTEN BRONZE THIN FILMS WITH OR WITHOUT TRANSITION METAL (Ag, Ti, Cr, Mn, Fe, Co, Ni and Cu) COATINGS.

Major Field: Chemistry

Biographical:

Personal Data: Born in, Multan, Punjab, Pakistan on April 20, 1975

Education: Graduated from Government College Sargodha, Punjab, Pakistan in July 1993; received a Bachelor of Science degree in Chemistry from University of the Punjab, Lahore, Pakistan in February 1999. Completed the requirements for the Masters of Science degree with a major in Chemistry at Oklahoma State University in May 2006.

Experience: Employed by University of the Punjab, Lahore Pakistan as an undergraduate research assistant, 1996-1999; Employed as a Lecturer in Chemistry at Multan Public School Multan from Jan 2000-Oct 2003;employed by Oklahoma State University, Department of Chemistry as a graduate teaching and research assistant, 2004 to present.

Professional Memberships: American Chemical Society, American Vacuum Society, Phi Lambda Upsilon Chemical Honorary Society.

Name: Kashif Rashid Khan Date of Degree: May, 2006

Institution: Oklahoma State University Location: Stillwater, Oklahoma

Title of study: PREPARATION AND NITROBENZENE REACTION KINETICS OF MICROCRYSTALLINE TUNGSTEN BRONZE THIN FILMS WITH OR WITHOUT TRANSITION METAL (Ag, Ti, Cr, Mn, Fe, Co, Ni and Cu) COATINGS.

Pages in Study: 53 Candidate for the Degree of Masters of Science

Major Field: Chemistry

Microcrystalline tungsten bronze (H_xWO_3) thin films are prepared using wet chemical techniques from tungsten oxide thin films. The oxide films are obtained by thermal oxidation of a sputter deposited tungsten metal film on a quartz substrate. X-ray photoelectron and visible spectroscopy results confirm that these films are indistinguishable from conventionally prepared tungsten bronze powders. The use of a quartz support allows the total amount of incorporated hydrogen in the film to be quantified by monitoring the absorbance at 900 nm. Once formed, the reduction kinetics of nitrobenzene and the concomitant oxidation of the tungsten bronze film are studied by measuring the absorption of 900 nm light as a function of time. By measuring the reaction rates on tungsten bronze films of various thicknesses a lower bound of 2×10^{-13} cm^2/sec is obtained for the hydrogen diffusion constant within the film. To increase the surface reaction rate, various transition metals (Ag, Ti, Cr, Mn, Fe, Co, Ni and Cu) are deposited on the surface using wet chemistry. By submerging tungsten bronze films in aqueous solutions of these transition metals, the bronze film will reduce the metal ions to form a metallic coating. For silver, deposition is controlled by submerging the films with different hydrogen concentrations in a silver nitrite solution and are quantified by the percent decrease in the absorbance of the films at 900 nm relative to the absorbance of freshly prepared bronze films. The fastest reduction rate of nitrobenzene is obtained from silver coating tungsten bronze films prepared from an uncoated bronze film whose absorbance at 900 nm has decayed to 75%-100% of its initial value. SEM and XPS studies of these films show that the even distribution of silver particles on the surface is responsible for the fast oxidation and reduction. In addition to silver, coated bonze films were prepared from the 1st row transition metals. In general, the reaction rate increases with atomic number toward a maximum around iron and then decreases. One exception to this general trend is the titanium coated bronze film. The reaction rate of these films exceeded that of all other transitions metals.

ADVISER'S APPROVAL: Dr. Nicholas F. Materer